land

MDPI

Communication

Impact of Climate Change on the Ground Thermal Regime in the Lower Lena Region, Arctic Central Siberia

Pavel Konstantinov [1,2,*], Nikolai Basharin [1,2], Alexander Fedorov [1], Yoshihiro Iijima [3], Varvara Andreeva [1,2], Valerii Semenov [1,2] and Nikolai Vasiliev [1,2]

[1] Permafrost Landscapes Laboratory, Melnikov Permafrost Institute of the Siberian Branch of the RAS, 677010 Yakutsk, Russia
[2] Laboratory for Integrated Research of the Arctic Land-Shelf System, Tomsk State University, 634050 Tomsk, Russia
[3] Graduate School of Bioresources, Mie University, 1577 Kurimamachiya-cho, Tsu 514-8507, Japan
* Correspondence: konstantinov@mpi.ysn.ru; Tel.: +7-924-868-58-05

Abstract: This paper presents the results of 30 years of permafrost thermal monitoring in the Tiksi area in the eastern Russian Arctic. At a stone ridge site, the mean annual temperatures in the upper 30 m of the ground have increased by 1–2.4 °C compared to the first years of observations, with trends of °C/yr. At the same time, its change was uneven. In the last 20 years, the rate of increase has increased compared with the first decade of observations. At wet tundra sites in the foothill plain, the mean annual temperatures at the top of permafrost have increased by 2.4–2.6 °C between 2005 and 2022 at rates of 0.11–0.15 °C/yr, and the active layer thicknesses have increased at rates of 0.05–0.41 cm/yr.

Keywords: climate change; permafrost; air temperature; ground temperature; active layer thickness

Citation: Konstantinov, P.; Basharin, N.; Fedorov, A.; Iijima, Y.; Andreeva, V.; Semenov, V.; Vasiliev, N. Impact of Climate Change on the Ground Thermal Regime in the Lower Lena Region, Arctic Central Siberia. *Land* **2023**, *12*, 19. https://doi.org/10.3390/land12010019

Academic Editor: Le Yu

Received: 20 November 2022
Revised: 9 December 2022
Accepted: 19 December 2022
Published: 21 December 2022

1. Introduction

In recent decades, air temperature in the Arctic has been increasing at about twice the global rate. This warming is expected to continue in the near future [1]. Warming in the Arctic has a significant impact on the structure and functioning of ecosystems, on the dynamics of carbon in the soil, and on infrastructure created by man. At the same time, all natural and manmade systems here are closely related to the state of permafrost. Continued warming processes in the Arctic may accelerate important feedback loops in permafrost degradation processes. Therefore, the study of permafrost and its thermal state is an important task for modern science.

The effects of climatic warming on permafrost are significant. Changes to the thermal condition of permafrost associated with the warming climate of the late 20th early 21st century have been well-documented in the Arctic regions of Asia and North America [2–22]. Despite the successful permafrost monitoring programs of recent years, it is critically important to establish new observatory sites and continue measurements at the existing sites. In 1992, the Melnikov Permafrost Institute, Yakutsk and the Institute of Low Temperature Science, Hokkaido University, Japan drilled a 30-m-deep borehole near the town of Tiksi in the eastern sector of the Russian Arctic and instrumented it for automated temperature data collection. Later, more monitoring sites were established for soil temperature and thaw depth measurements. The results from these observations are discussed in this paper.

2. Study Area

The study area is located in the eastern foothills of the Primorsky Range which extends on into the seacoast near the town of Tiksi. The Primorsky Range is a far northeastern part of the Kharaulakh Low Mountain System. The ridge is heavily dissected and has bald, flattened tops. Elevations range from 100 to 300 m a.s.l. The valleys are predominantly

U-shaped. The geology of the Primorsky Range near Tiksi consists of Carboniferous and Permian rocks. The foothills are composed of sedimentary rocks of the Lower Carboniferous Tiksi Formation, which is Namurian in age. This unit conformably overlies the continental sediments of Visean age and consists of black siltstone, argillite and marl containing limestone interbeds [23]. Bedrock near the surface is closely jointed. Quaternary sediments are thin throughout the area and do not exceed 1.5–2 m in thickness. Nival weathering and associated slope deposits predominate in the upper and middle belts of the mountains. Most common processes in the foot slope zone are solifluction and proluvial action causing torrential washing of fine materials. They form extensive cones which in places overlie the alluvium in the valleys. The alluvium consists of thin (0.5–1.5 m) floodplain and low-terrace deposits.

The Tiksi area lies in the excessively wet climatic zone with cold, low snow winters and cool summers [24]. During the 2010–2021 period, mean monthly air temperatures at the Tiksi meteorological station ranged between −25.6 and −34 °C in January and between +6.3 and +12.6 °C in July. The mean daily air temperature falls below 0 °C in late September–early October and rises above 0 °C in early June. Frosts in the surface air and in the soil occur any month in the summer. The warmest period is from the second half of July through the first half of August. The incoming solar radiation is 2950–3150 MJ m^2 yr, and the net radiation is 600 MJ m^2 yr [25]. The annual precipitation in 2010–2021 ranged from 172 to 349 mm, most of which occurred during the summer (June to September). The precipitation exceeds the evaporation. The number of days with snow cover is up to 260 days. A permanent snow cover is established in early October and melts in early June. Snow on the ground surface is redistributed by high winds (up to 20 m/s), resulting in snow depth variation across the landforms. The tops of the hills and stone ridges, as well as the hillocks in the foothill plain have a very thin snow cover or blown entirely free of snow. Snow is collected on the lee foot slopes, as well as on thermokarst depressions in the foothill plain. Wind-blown snowbanks are formed occasionally at the foot of altiplanation terraces, which persist until the end of the summer season.

Vegetation is dominated by mountain tundra and wet tundra communities. Arctic desert and valley communities are less common [26].

Permafrost is continuous in the study area. It is characterized by cold temperatures and a thin active layer. The geothermal heat flux in the Tiksi area is in the range from 50 to 60 mWt/m^2 [27]. In 1962, permafrost temperature measurements were taken to a depth of 500 m in the Tiksi Bay area (Table 1). The permafrost thickness was estimated by extrapolation to be 640 m [28]. The depth of seasonal thawing is shallow owing to the severe climatic conditions. According to the Active-Layer Map of Yakutia, typical average values of the active layer thickness in the study area are 25 cm in peat, 30 cm in silty clay and silty sand with an upper peat horizon, 40 cm in silty clay and clay with no peat horizon, 80 cm in sand and sandy silt with no peat horizon, and up to 100 cm in gravels and boulders without a peat horizon [29]. A variety of frost-related processes and features occur in the region, including patterned ground features resulting from frost heaving, ground wedge and ice-wedge polygons associated with thermal contraction cracking, and thermokarst and thermal abrasion related to partial thawing of permafrost. Solifluction is observed in the foot slope areas.

Table 1. Permafrost temperatures in the Tiksi Bay area measured in January–February 1962 [28].

Depth, m	Temperature, °C
20	−11.1
100	−10.5
200	−8.6
300	−6.8
400	−4.8
500	−2.9

3. Monitoring Sites and Methods

The study sites are located in the lower part of the Suonannakh Creek valley, 5 km southwest of Tiksi (Figure 1). This area lies in a foothill zone of the Primorsky Range with the topography consisting of low mountains and stone ridges covered by mountain tundra, gentle hillslopes, and a foothill plain dissected by stream valleys and covered by wet tundra. Long-term ground temperature monitoring is conducted at three sites, and active-layer thickness measurements are taken annually at the end of summer season at 10 points located in the foothill plain.

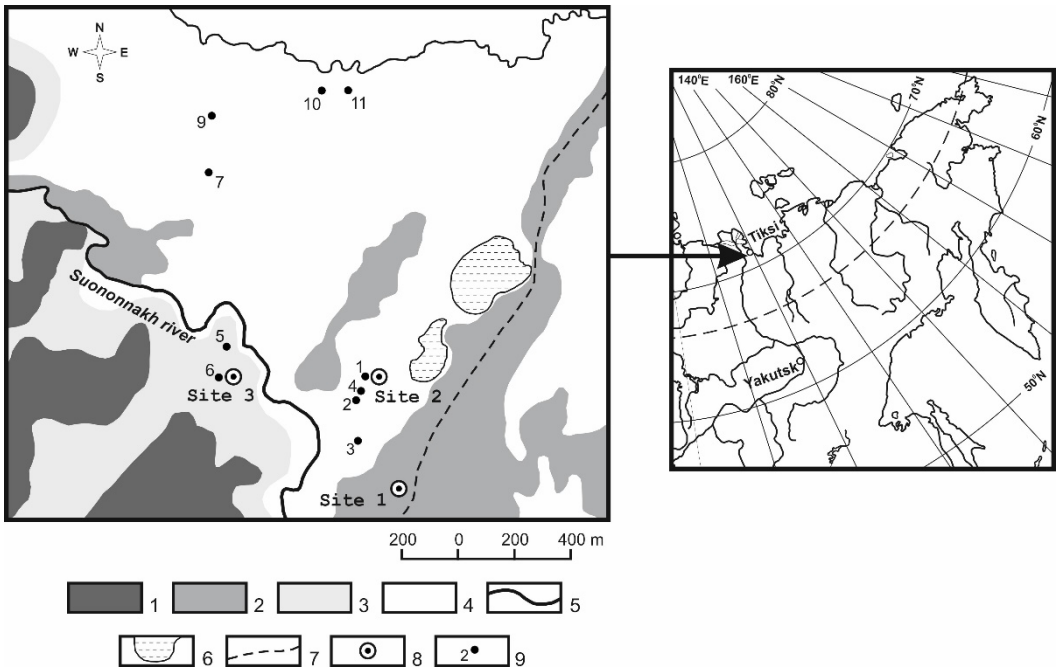

Figure 1. Map of the study area. 1—hills; 2—stone ridges; 3—gentle slopes; 4—foothill plain; 5—streams; 6—lakes; 7—road; 8—ground temperature monitoring sites; 9—active-layer measurement sites.

Site 1 is situated near the summit of a stone ridge rising 8–10 m above the surrounding foothill plain (Figure 2). The site surface is blanketed by platy fragments of argillite. A previous study characterized the vegetation as graminoid (*Poa alpigena*), clastic mountain tundra [26]. *Poa alpigena* covers less than 20% of the area. The grass cover also contains sparse *Gastrolychnis apetala* and *Artemisia leocophilla*. In the summer of 1992, a 30-m deep borehole was drilled at the site. The drilling data showed that the upper 4 m of subsurface material consist of platy fragments of argillite. This layer is underlain, to a depth of 30 m, by a fissured mass of argillite with varying degrees of weathering. The borehole was instrumented with platinum resistance thermometers placed at depths of 0, 1, 2, 3, 5, 10, 20 and 30 m. After installing the temperature cable, the borehole was entirely backfilled with fine rock fragments. A metal box was placed on the top of the casing tube to house the DATAMARK LS-3300PtV temperature data logger (HAKUSAN, Japan). Temperatures are recorded every 12 h. Data have been retrieved once a year, at the end of the thaw season, since 1993. In 2013 this temperature borehole was registered in the database of the international project "Global Terrestrial Network for Permafrost" (GTN-P).

Site 2 is located in the foothill plain, 400 m north of Site 1. The landscape consists of flat hillocky wet tundra (Figure 3). The hillocks are covered entirely by green mosses (*Polytrichum hyperboreum, Aulacomnium turgidum, Dicranum elognatum*) and partially by lichens (*Cetraria cucullata*). The moss and peat layer is 15–20 cm thick. The mineral soils consist of clay-rich silts and clays. The grain-size distribution and physical properties of the soils at Site 2 are given in Tables 2 and 3. The bog hollows which occupy up to 40% of

the area, support *Carex concolar* and *Eriophorum polystachion* bogs [26]. The bog hollows are very wet but contain no open water. The ALT varies interannually from 30 to 45 cm in the hillocks and from 35 to 55 cm in the bog hollows. In summer 2004, Site 2 was instrumented with a single-channel TR-52 data logger (T&D Corporation, Nagano, Japan) for hourly measurements of temperature at the top of permafrost. The temperature sensor is placed at a depth of 0.6 m. The annual data are retrieved at the end of the thaw season (September).

Figure 2. General view of monitoring site 1.

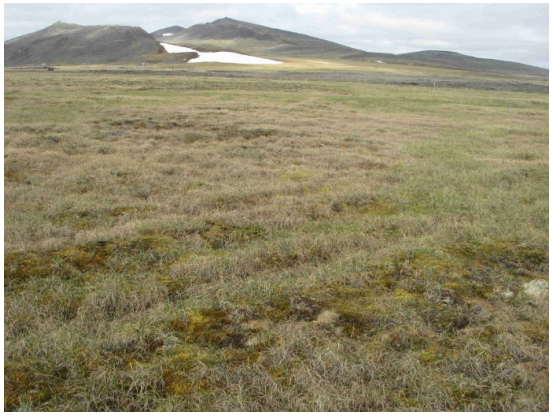

Figure 3. General view of monitoring site 2.

Table 2. Grain-size distribution of the mineral soil, Site 2.

Granulometric Composition, % (to Fractions, mm)	Depth, m				
	0.20–0.30	0.20–0.30	0.25–0.30	0.25–0.30	0.25–0.30
10–7	3	-	-	-	-
7–5	-	-	-	-	-
7–3	-	-	-	-	-
3–2	-	-	-	-	-
2–1	-	-	-	-	-
1–0.5	-	-	-	-	-
0.5–0.25	3	1.4	1.1	1.1	1.4
0.25–0.19	7	4.6	6.5	6.7	9.8
0.10–0.05	0.6	17	8.2	7.7	9.4
0.05–0.01	19.5	15	28.4	29.9	32
0.01–0.005	31.5	22.1	22.4	20.6	14.9
0.005–0.002	6.8	7.8	7.4	2.9	6.2
<0.002	28.6	32.1	26.2	31.1	26.3
	Clay loam	Clay	Clay loam	Clay	Clay loam

Table 3. Physical properties of the soil horizons, Site 2.

Depth, cm	Soil Composition	Gravimetric Moisture Content, %	Volumetric Moisture Content, %	Bulk Density of humid Soil, g/cm^3	Bulk Density of Dry Soil, g/cm^3
10	Peat	157	72	1.18	0.46
12	Peat	190	74	1.14	0.39
15	Peat	158	74	1.20	0.47
16	Peaty soil	61	56	1.48	0.92
17	Peaty soil	95	60	1.23	0.63
17	Peaty soil	68	58	1.43	0.85
20	Clay soil	37	47	1.74	1.27
23	Clay soil	39	48	1.69	1.22
25	Clay soil	36	48	1.80	1.33
27	Clay soil	29	41	1.82	1.41

Site 3 is 500 m west of Site 2. It is located at the base of a gentle slope (Figure 4). The landscape is hillocky wet tundra. The hillocks are covered by a continuous layer of green mosses (*Dicranum elognatum*, *Polytrichum alpinum*) and partially by lichens (*Cetraria cucullata*, *Cladina arbuscula*). The moss and peat layer is 20 to 25 cm thick. *Carex concolar*, *Eriophorum polystachion* and *Sphagnum warnstorfii* bog communities occupy the bog hollows [26]. The ALT values vary from year to year between 25 and 40 cm. In 2004, the site was instrumented with a TR-52 data logger with its temperature sensor placed at 0.5 m depth. Temperature data retrieval is similar to that at Site 2.

Figure 4. General view of monitoring site 3.

Starting from 2006, ALT measurements have been made at 10 permanent points set up in the wet tundra foothill plain (see Figure 1). Hand probing with a metallic rod is done each September at the points marked with stakes. At each point, at least three measurements are taken at a distance of 10–15 cm from the stake base.

Snow depths were measured in some years during the period of maximum snow accumulation (March–April). Additionally, data on air temperature, precipitation, and snow depth and density from the Tiksi meteorological station have been used in this study. The station operated by the Russian Service for Hydrometeorology and Environmental Monitoring is located 5 km east of the monitoring sites.

4. Results and Discussion

In this study, mean annual ground temperature (MAGT) and mean annual air temperature (MAAT) were calculated for a "geocryological" year rather than a calendar year. A.V. Pavlov [30] defines it as a 12-month period which begins with the long-term average start

of soil freezing which corresponds to the onset of consistently subzero soil surface temperatures. In this case, the cold season, including the entire snow season, falls within one year. This approach is more appropriate for permafrost regions where the ground thermal regime is more dependent on winter than on summer conditions. In the study area, the soil surface temperature falls below 0 °C in late September or early October. For convenience, MAGT and MAAT were calculated for a year from October 1 of the preceding year through September 30 of the given year. For example, MAGT and MAAT for 2013 are the values calculated for the annual period extending from 1 October 2012 to 30 September 2013.

Figure 5 shows the change in MAAT from 1991 to 2021. Its upward trend was 0.11 °C/yr. At the same time, the change in MAAT occurred unevenly. This can be seen from Table 4, where presents the 5-year averages of mean monthly and annual air temperatures at the Tiksi station for the 1991–2021 period. Since about the middle of the first decade of the 21st century, the rate of increase in air temperature has increased markedly. The long-term increase in air temperature varied between months. The increase was larger for October, November, March, April, June, August, and September. The coldest months (December–February), as well as May and July experienced much smaller increases.

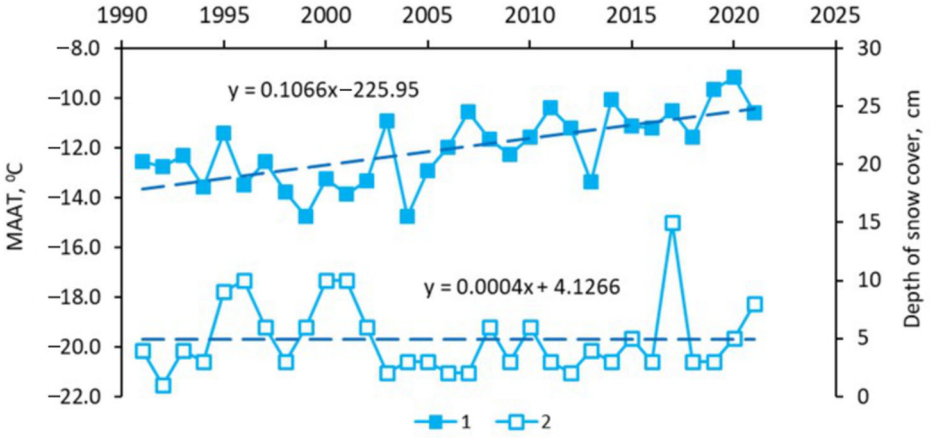

Figure 5. Mean annual air temperature (1) and maximum snow depth (2) in 1991–2021 for the Tiksi station.

Table 4. Five-year averages of the mean monthly and annual air temperatures in 1991–2021 for the Tiksi meteorological station.

Month	1991–1995	1996–2000	2001–2005	2006–2010	2011–2015	2015–2021
Oct.	−10.8	−10.7	−11.9	−9.0	−8.8	−7.5
Nov.	−25.6	−24.4	−22.8	−21.7	−19.9	−19.4
Dec.	−27.8	−30.0	−29.5	−26.9	−26.8	−27.8
Jan.	−30.3	−30.9	−30.3	−26.9	−30.3	−29.0
Feb.	−27.5	−29.8	−33.0	−31.4	−31.4	−28.1
Mar.	−25.8	−29.4	−26.4	−25.5	−23.5	−22.5
Apr.	−18.7	−18.7	−18.4	−17.6	−14.8	−13.4
May	−5.4	−6.4	−6.3	−4.3	−4.4	−5.5
June	3.3	3.0	2.7	4.3	4.0	5.7
July	8.7	7.3	8.5	8.3	9.0	8.8
Aug.	7.6	6.9	8.1	9.0	9.3	9.3
Sept.	2.0	0.5	1.4	2.4	3.0	3.9
MAAT (°C)	**−12.5**	**−13.6**	**−13.2**	**−11.6**	**−11.2**	**−10.5**

Snow depth data for the Tiksi station show little variation between 1991 and 2021 (a trend of 0.0004 cm/yr) [see Figure 5].

Figure 6 shows the mean annual, minimum, and maximum ground temperate profiles at Site 1 (stone ridge) for 1992–1993 and 2021–2022. Compared to the early monitoring years,

the recent MAGT values are higher by 1.7 °C at the depth of 3 m, 2.4 °C at 5 m, 1.9 °C at 10 m, and 1.0 °C at 30 m. As seen from the plots, the initial temperature profile in the 0–30 m depth interval, which was isothermal at the start of monitoring, is becoming degradational. Similar forms of temperature curves in the depth interval of 0–27 m were obtained from studies on Samoilovsky Island in the delta of the Lena River in 2006–2017 [31].

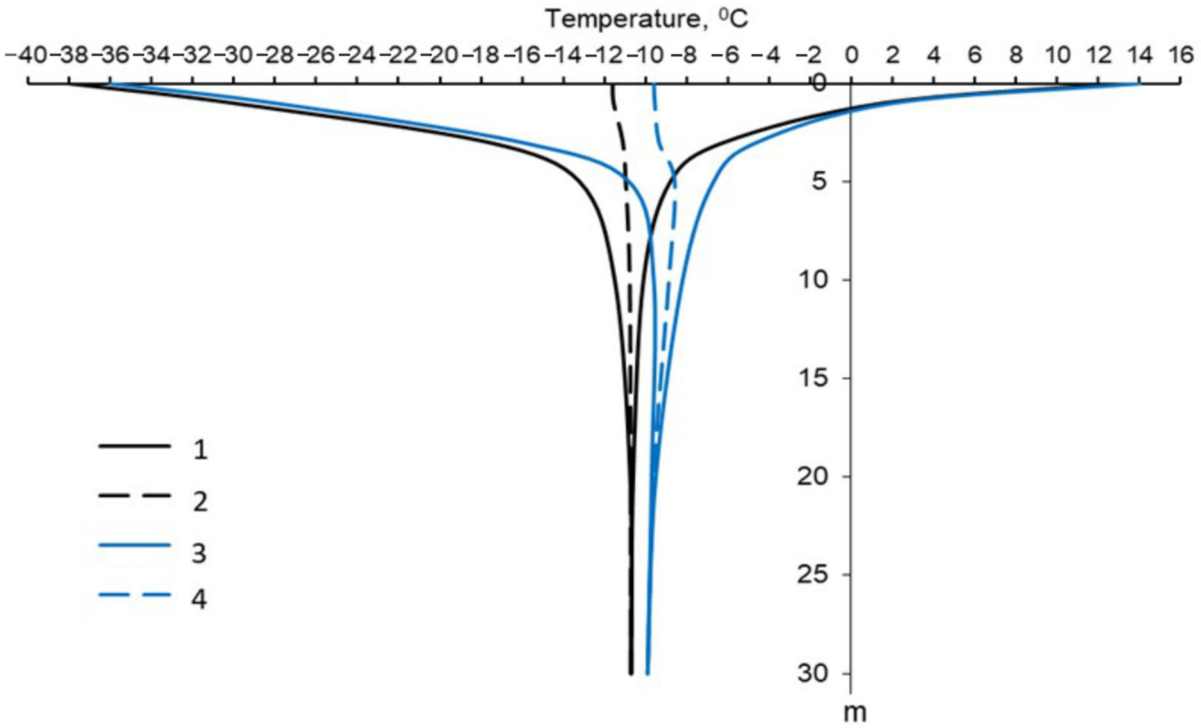

Figure 6. Temperature profiles from the 30-m borehole in the stone ridge (Site 1) for 1992–1993 and 2021–2022. 1—minimal and maximum temperatures in 1992–1993; 2—mean annual temperatures in 1992–1993; 3—minimal and maximal temperatures in 2021–2022; 4—mean annual temperatures in 2021–2022.

Figure 7 presents the interannual MAGT variations at depths of 3, 10, and 30 m for Site 1 (stone ridge). For the entire period of observations (1993–2022) the trends of its increase were respectively 0.10, 0.08, and 0.04 °C/yr. Additionally, MAGT trends were calculated over decades (Table 5). As with MAAT (see Table 4), the change in MAGT was uneven. In 1993–2002 at depths of 3 and 10 m, there was a tendency even for its slight decrease. In 2003–2012 and 2013–2022 at all depths, there was a tendency for a significant increase in MAGT at all depths. It should be noted that air temperature is the single most important factor controlling the permafrost temperature dynamics in the study area. The insulating effect of snow cover is limited because of the climatic and terrain conditions. Strong wind action results in high density of snow cover, which increases from 190–200 kg/m^3 in the early winter (October–November) to as much as 250–350 kg/m^3 by the late winter. In addition, snow cover is thin where snow is blown away. At Site 1, for example, the late winter snow depth ranges within 2–20 cm from year to year.

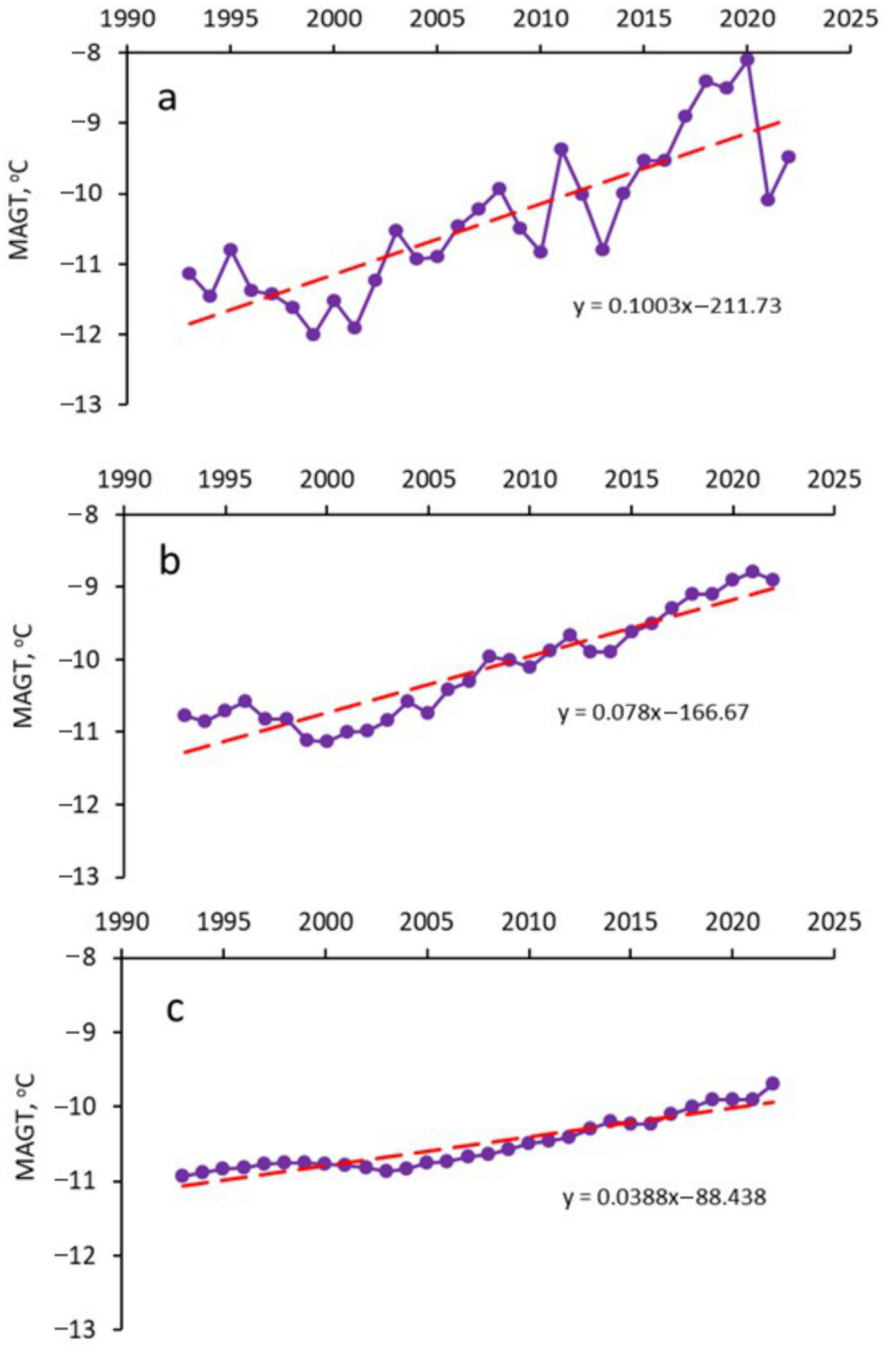

Figure 7. Mean annual permafrost temperature in the stone ridge (Site 1) at depths of 3 m (**a**), 10 m (**b**) and 30 m (**c**) in 1993–2022.

Table 5. Trends in the MAGT for the entire period and for decades at the stone ridge. (Site 1).

Years	MAGT Trends (°C/yr)		
	3 m	**10 m**	**30 m**
1993–2022	0.10	0.08	0.04
1993–2002	−0.06	−0.04	0.01
2003–2012	0.10	0.12	0.05
2013–2022	0.13	0.13	0.06

Figure 8 illustrates the variation in mean annual ground temperature at the top of permafrost ($MAGT_{PT}$) at Sites 2 and 3 covered by wet-tundra communities. As the sites were instrumented in 2004, the $MAGT_{PT}$ data are only available for the period of increasing MAAT. In the foothill plain covered by flat hillocky wet tundra (Site 2), $MAGT_{PT}$ increased by 2.6 °C between 2005 and 2022 (a trend of 0.15 °C/yr). At the foot of a gentle hillslope covered by hillocky wet tundra (Site 3), $MAGT_{PT}$ increased by 2.4 °C over the same period (a trend of 0.11 °C/yr).

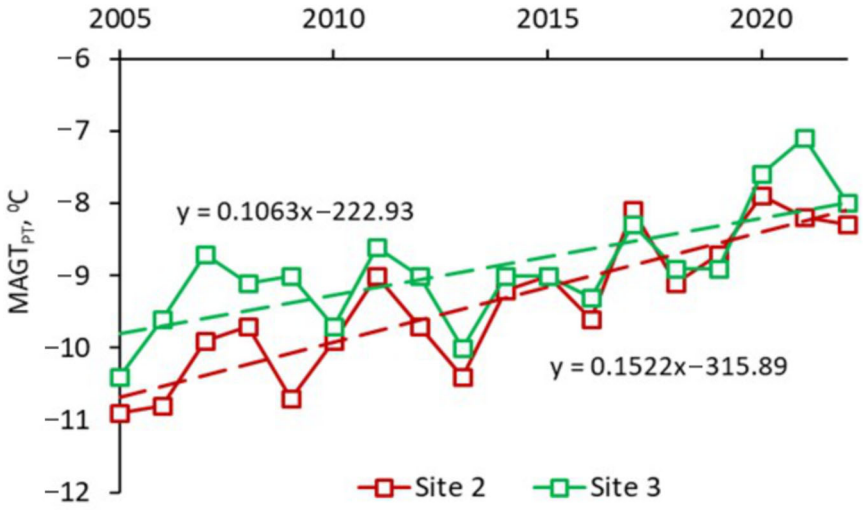

Figure 8. Mean annual temperature at the top of permafrost in the wet tundra areas (Sites 2 and 3), 2005–2022.

Starting from 2006, active layer thickness (ALT) have been measured at 10 fixed points set up at the wet tundra locations. ALT is an important characteristic of the thermal state of permafrost. Its increase is one of the indicators of climate warming processes. The growth of ALT may cause the development of thermokarst, an increase in the emission of greenhouse gases into the atmosphere, and other changes in the Arctic ecosystems. According to the landscape features, monitoring points of the ALT study are classified into three groups: 1) flat moss hillocks in sub-horizontal areas of the foothill plain (points 4, 7 and 10); 2) bog hollows in sub-horizontal areas of the foothill plain (points 1, 2, 3, 8 and 9); and 3) moss hillocks at the foot of gentle hillslopes (points 5 and 6). The vegetation characteristics of the ALT sites are given in the description of monitoring sites 2 and 3. Figure 9 plots the variation in ALT over the observation period 2006–2022 for the above three groups. The increase in ALT was, on average, 5.3 cm (trend 0.33 cm/yr) for the first group, 6.6 cm for the second group (trend 0.41 cm/yr), and only 0.8 cm (trend 0.05 cm/yr) for the third group. Figure 10 shows the change in the thawing index, which reflects the thermal resources of the summer period. According to the Tiksi meteorological station, in 2006–2022 it increased with a trend of 13 degree-days/year. Based on this, ALT increase can be explained by an increase in the thermal resources of the summer period in 2006–2022 against the background of an increase in the temperature of permafrost. In 2006–2022 a decrease in summer precipitation was observed in the Tiksi region (Figure 11), which apparently has little effect on ALT fluctuations here. This can be explained by the water-saturated state of tundra-marsh soils, regardless of interannual fluctuations in the amount of rainfall.

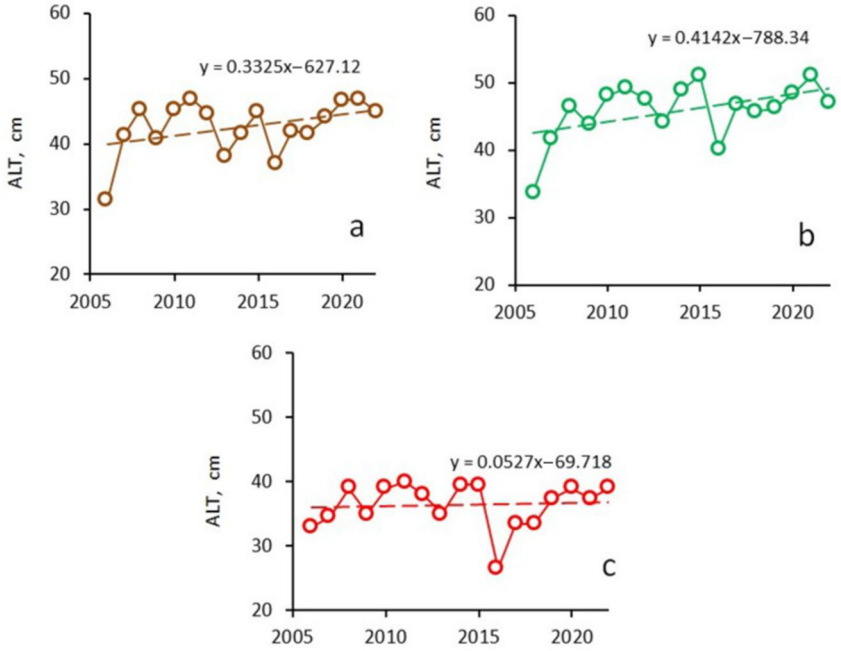

Figure 9. Active layer thickness in the wet-tundra sites, 2006–2022. (**a**)—flat moss hillocks in sub-horizontal areas of the foothill plain; (**b**)—swales in horizontal areas of the foothill plain; (**c**)—moss hillocks in the gentle lower hillslopes.

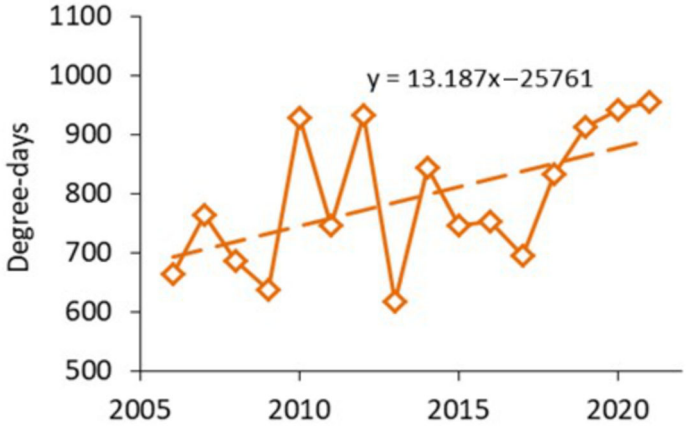

Figure 10. Air thawing index (June-September) for the Tiksi station, 2005–2022.

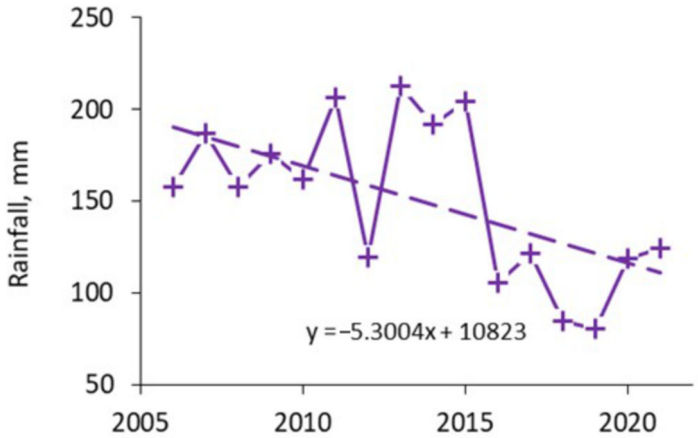

Figure 11. Rainfall amounts for the Tiksi station, 2005–2022.

It is of interest to compare our results with other permafrost thermal investigations in the region. One location nearby is the Samoylov Research Station in the Lena Delta, 110 km north-west of Tiksi. In 2006, the joint Russian–German field team drilled and instrumented a 27-m-deep thermal borehole on Samoylov Island [32]. The initial MAGTs were −8.6, −8.9 and −8.9 °C at the depths of 10, 20 and 27 m, respectively. For comparison, the MAGTs in 2006 measured in the borehole near Tiksi were −10.3, −10.3 and 10.7 °C at the depths of 10, 20 and 30 m, respectively. As is seen, the permafrost temperatures were colder in the rocks near Tiksi compared to the Lena River alluvium on Samoylov Island. This can be explained by the warming effect of a large river on the permafrost within the river islands. Between 2008 and 2016, the MAGT at 20 m depth increased by 0.9 °C on Samoylov Island [16]. Near Tiksi, the increase in MAGT at 20 m depth was smaller over the same period, comprising 0.6 °C. Such differences are quite acceptable, considering the different geological structure and different landscape conditions of the compared experimental sites.

Thanks to the international project GTN-P, it became possible to obtain global estimates of the thermal state of permafrost. Biskaborn et al. [16] analyzed a global set of permafrost temperatures near a depth of zero annual amplitude to evaluate the thermal state of permafrost for the period since the International Polar Year (2007–2009). They found that the average temperature increase for the Arctic during the decade between 2007 and 2016 was 0.39 ± 0.15 °C. The permafrost temperatures near Tiksi and on Samoylov Island increased by 0.6 and 0.9 °C respectively during this period, exceeding the average permafrost warming in the Arctic.

5. Conclusions

1. At the stone ridge site, the mean annual ground temperature was higher by 1.7 °C at 3 m, 2.4 °C at 5 m, 1.9 °C at 10 m, and 1.0 °C at 30 m depth in 2022, compared with the first year of monitoring. Over the 30 year observation period (1993–2022), the trending increase amounted to 0.04–0.10 °C/yr. At the same time, the change in MAGT occurred unevenly. In the last 20 years, the rate has increased compared to the first decade of observations. Comparison of our results to the reported global-scale analysis of the thermal state of permafrost for 2007–2016 shows that the permafrost temperature increase in the lower Lena region exceeds the average increase for the Arctic zone.

2. At the wet tundra sites in the foothill plain, the mean annual temperature at the top of permafrost has increased by 2.4–2.6 °C between 2005 and 2022 at rates of 0.11–0.15 °C per year. From 2005 to 2022, the active layer thickness increased, with trends of 0.05–0.41 cm per year, due to the increased summer heat resources in 2006–2022 with a simultaneous increase in permafrost temperature.

Author Contributions: Conceptualization, P.K.; methodology, P.K.; validation, P.K., Y.I. and A.F.; formal analysis, P.K.; investigation, P.K., N.B., A.F., Y.I., V.A., V.S., N.V.; resources, P.K.; data curation, P.K.; writing—original draft preparation, P.K.; writing—review and editing, P.K.; visualization, P.K.; supervision, P.K.; project administration, P.K.; funding acquisition, P.K. All authors have read and agreed to the published version of the manuscript.

Funding: This study was basically supported by the Russian Ministry of Science and Higher Education (Grant "Priority-2030" to Tomsk State University) and RMSHE (AAAA-A20-120111690009-6 "Cryogenic Processes and Natural Risks Associated with the Development of Permafrost Landscapes in Eastern Siberia"). We also thank RFBR for their partial support (projects: 19-29-05151, 20-55-71005, 21-55-75004).

Data Availability Statement: The data presented in this study are available on request from the corresponding author.

Conflicts of Interest: The authors declare no conflict of interest.

References

1. ACIA. *Arctic Climate Impact Assessment Cambridge*; Cambridge University Press: Cambridge, UK, 2005; p. 1042.
2. Romanovsky, V.E.; Sazonova, T.S.; Balobaev, V.T.; Shender, N.I.; Sergueev, D.O. Past and recent changes in air and permafrost temperatures in Eastern Siberia. *Glob. Planetary Chang.* **2007**, *56*, 399–413. [CrossRef]

3. Osterkamp, T.E. Thermal state of permafrost in Alaska during the fourth quarter of the twentieth century. In *Proceedings of the Ninth International Conference on Permafrost*; Kane, D.L., Hinkel, K.M., Eds.; Institute of Northern Engineering, University of Alaska: Fairbanks, AK, USA, 2008; Volume 2, pp. 1333–1338.
4. Smith, S.L.; Romanovsky, V.E.; Lewkowicz, A.G.; Burn, C.R.; Allard, M.; Clow, G.D.; Yo-shikawa, K.; Throop, J. Thermal state of permafrost in North America: A contribution to the international Polar year. *Permafr. Perigl. Process.* **2010**, *21*, 117–135. [CrossRef]
5. Romanovsky, V.E.; Drozdov, D.S.; Oberman, N.G.; Malkova, G.V.; Kholodov, A.L.; Marchenko, S.S.; Moskalenko, N.G.; Sergeev, D.O.; Ukraintseva, N.G.; Abramov, A.A. Thermal state of permafrost in Russia. *Permafr. Perigl. Process.* **2010**, *21*, 136–155. [CrossRef]
6. Romanovsky, V.E.; Smith, S.L.; Christiansen, H.H. Permafrost thermal state in the polar Northern Hemisphere during the international polar year 2007–2009: A synthesis. *Permafr. Perigl. Process.* **2010**, *21*, 106–116. [CrossRef]
7. Romanovsky, V.; Smith, S.; Isaksen, K.; Shiklomanov, N.I.; Streletskiy, D.A.; Kholodov, A.L.; Khoshkam, M.; Kidd, R.; Killick, R.; Kim, H.; et al. Terrestrial permafrost. In: State of the Climate in 2018. *Bull. Am. Meteorol. Soc.* **2019**, *100.9*, 153–156.
8. Vasiliev, A.A.; Streletskaya, I.D.; Shirokov, R.S.; Oblogov, G.E. Coastal permafrost evolution of Western Yamal in context of climate change. *Eart Cryosphere* **2011**, *2*, 56–64. (In Russian)
9. Vasiliev, A.A.; Drozdov, D.S.; Gravis, A.; Malkova, G.; Nyland, K.E.; Streletskiy, D.A. Permafrost degradation in the Western Russian Arctic. *Environ. Res. Lett.* **2020**, *10*, 045001. [CrossRef]
10. Kraev, G.; Abramov, A.; Bykhovets, S.; Fyodorov-Davydov, D.; Kholodov, A.; Lupachev, A.; Mamykin, V.; Ostroumov, V.; Sorokovikov, V.; Gilichinsky, D.; et al. Ther-mal State of Permafrost in the Eastern Arctic. In *Tenth International Conference on Permafrost*; Kane, D.L., Hinkel, K.M., Eds.; Institute of Northern Engineering, University of Alaska Fairbanks: Fairbanks, AK, USA, 2012; Volume 1, pp. 993–998.
11. Malkova, G.V. The Last Twenty-Five Years of Changes in Permafrost Temperature in the Eu-ropean Russian Arctic. In *Tenth International Conference on Permafrost*; Kane, D.L., Hinkel, K.M., Eds.; Institute of Northern Engineering, University of Alaska Fairbanks: Fairbanks, AK, USA, 2012; Volume 2, pp. 1119–1124.
12. Way, R.G.; Lewkowicz, A.G. Environmental controls on ground temperature and permafrost in Labrador, 576 northeast Canada. *Permaf. Perigl. Process.* **2018**, *29*, 73–85. [CrossRef]
13. Westergaard-Nielsen, A.; Karami, M.; Hansen, B.U.; Westermann, S.; Elberling, B. Contrasting temperature trends across the ice-free part of Greenland. *Sci. Rep.* **2018**, *8*, 1586. [CrossRef] [PubMed]
14. Abramov, A.; Davydov, S.; Ivashchenko, A.; Karelin, D.; Kholodov, A.; Kraev, G.; Lupachev, A.; Maslakov, A.; Ostroumova, V.; Rivkina, E.; et al. Two Decades of Active Layer Thickness Monitoring in Northeastern Asia. *Polar Geogr.* **2019**, *44*, 186–202. [CrossRef]
15. Dubrovin, V.A.; Brushkov, A.V.; Drozdov, D.S.; Zheleznyak, M.N. Study, current state, future and challenges of development of permafrost in the Arctic. In *Mineralnye Resursy Rossii. Ekonomika i Upravlenie*; PravoTEK: Moscow, Russia, 2019; Volume 3, pp. 55–64. (In Russian)
16. Biskaborn, B.K.; Smith, S.L.; Noetzli, J.; Matthes, H.; Vieira, G.; Streletskiy, D.A.; Schoeneich, P.; Romanovsky, V.E.; Lewkowicz, A.G.; Abramov, A.; et al. Permafrost is warming at a global scale. *Nat. Commun.* **2019**, *10*, 264. [CrossRef] [PubMed]
17. Wang, C.; Wang, Z.; Kong, Y.; Zhang, F.; Yang, K.; Zhang, T. Most of the Northern Hemisphere Permafrost Remains under Climate Change. *Sci. Rep.* **2019**, *9*, 3295. [CrossRef] [PubMed]
18. Zhelezniak, M.N.; Semenov, V.P. *The Subsurface Temperature Field and Permafrost in the Vilyui Basin*; SB RAS: Novosibirsk, Russia, 2020; 123p. (In Russian)
19. Kaverin, D.; Malkova, G.; Zamolodchikov, D.; Shiklomanov, N.; Pastukhov, A.; Novakovskiy, A.; Sadurtdinovb, M.; Skvortsov, A.; Tsarev, A.; Pochikalovg, A.; et al. Long-Term Active Layer Monitoring at CALM Sites in the Russian European North. *Polar Geogr.* **2021**, *44*, 203–216. [CrossRef]
20. Strand, S.M.; Christiansen, H.H.; Johansson, M.; Åkerman, J.; Humlum, O. Active layer thickening and controls on interannual 568 variability in the Nordic Arctic compared to the circum-Arctic. *Permafr. Perigl. Process.* **2021**, *32*, 47–58. [CrossRef]
21. Li, G.; Zhang, M.; Pei, W.; Melnikov, A.; Khristoforov, I.; Li, R.; Yu, F. Changes in permafrost extent and active layer thickness in the Northern Hemisphere from 1969 to 2018. *Sci. Total Environ.* **2022**, *804*, 150182. [CrossRef] [PubMed]
22. Ran, Y.; Li, X.; Cheng, G.; Che, J.; Aalto, J.; Karjalainen, O.; Hjort, J.; Luoto, M.; Jin, H.; Obu, J.; et al. New high-resolution estimates of the permafrost thermal state and hydrothermal conditions over the Northern Hemisphere. *Earth Syst. Sci. Data* **2022**, *14*, 865–884. [CrossRef]
23. *Geology of the Yakutian ASSR*; Spektor, V.B. (Ed.) Nedra: Moscow, Russia, 1981; 300p. (In Russian)
24. Budyko, M.I.; Grigoriev, A.A. Climatic zonation of the USSR. In *The Climatic Atlas of the USSR*; Gl. Upr. Gidrometeorol. Sluzhby pri Sovmine SSSR: Moscow, Russia, 1960; Volume 1, pp. 178–179. (In Russian)
25. *The Atlas of the USSR*; GUGK: Moscow, Russia, 1984; 260p. (In Russian)
26. Desyatkin, R.V.; Karpov, N.S.; Zakharova, V.I.; Desyatkin, A.R.; Hinzmann, L.D. Soil and vegetative covers on tundra polygon of the GAME project in the vicinity of Tiksi. Research Re-port of IHAS. In *Proceedings of Second International Workshop of Energy and Water Cycle in GAME-Siberia*; Institute for Hydrospheric-Atmospheric Sciences: Nagoya, Japan, 1998; Volume 4, pp. 1–10.
27. Balobaev, V.T. *Geothermy of the Permafrost Zone of the Lithosphere in Northern Asia*; Nauka: Novosibirsk, Russia, 1991; p. 194. (In Russian)
28. Grigoriev, N.F. *Permafrost in the Coastal Zone of Yakutia*; Nauka: Moscow, Russia, 1966; p. 180. (In Russian)

29. Soloviev, P.A. Thickness of the surficial seasonally frozen layer in Yakutian ASSR. In *Geocryological and Hydrogeological Investigations in Yakutia*; Kn. Izdatelstvo: Yakutsk, Russia, 1978; pp. 3–12. (In Russian)
30. Pavlov, A.V. *Heat Exchange of Freezing and Thawing Soils with the Atmosphere*; Russian Academy of Sciences: Moscow, Russia, 1965; p. 254. (In Russian)
31. Boike, J.; Nitzbon, J.; Anders, K.; Grigoriev, M.; Bolshiyanov, D.; Langer, M.; Lange, S.; Bornemann, N.; Morgenstern, A.; Schreiber, P.; et al. A 16-year record (2002–2017) of permafrost, active layer, and meteorological conditions at the Samoylov Island Arctic permafrost research site, Lena River Delta, northern Siberia: An opportunity to validate remote sensing data and land surface, snow, and permafrost models. *Earth Syst. Sci. Data Discuss.* **2018**, *11*, 261–299. [CrossRef]
32. Boike, J.; Kattenstroth, B.; Abramova, K.; Bornemann, N.; Chetverova, A.; Fedorova, I.; Fröb, K.; Grigoriev, M.N.; Grüber, M.; Kutzbach, L.; et al. Baseline characteristics of climate, permafrost and land cover from a new permafrost observatory in the Lena River Delta, Siberia (1998–2011). *Biogeosciences* **2013**, *10*, 2105–2128. [CrossRef]